

## Hydrogen Production via Chemical Looping Reforming Using $\text{Fe}_2\text{O}_3$ as Oxygen Carrier

F. Mahmoodi<sup>1</sup>, S.H. Najibi<sup>1</sup>, A. Shariati\*<sup>2</sup>

<sup>1</sup>.Department of Chemical Engineering, Petroleum University of Technology, Ahwaz, Iran

<sup>2</sup>.Department of Chemical Engineering, Petroleum University of Technology, Ahwaz 6198144471, Iran

[Shariati@put.ac.ir](mailto:Shariati@put.ac.ir)

**Abstract:** Hydrogen is known a clean and efficient alternative for the future. Since water is its only combustion product, it has almost no negative effect on environment. Currently, most of hydrogen produced at an industrial scale is obtained by natural gas reforming. However, it must be purified in a downstream process to be used for other applications (e.g. in fuel cell). Alternatively, pure hydrogen can be produced from hydrogen containing compounds such as fossil fuel and water in other processes. Chemical looping reforming is such a process that can be used for pure hydrogen production with inherent  $\text{CO}_2$  capture. It involves the use of metal oxide as oxygen carrier, which transfers oxygen from steam to the fuel. In the present study, a water gas shift reaction (WGS) using chemical looping technology was studied. Specifically, the  $(\text{Fe}_2\text{O}_3\text{-CeO}_2)$  as oxygen carrier was prepared by co-precipitation of nitrate compounds of Fe and Ce. It was characterized using X-ray diffractometer (XRD) and (XRF), scanning electron microscope (SEM), BET and hydrogen programmed reduction ( $\text{H}_2$ -TPR) techniques. The reactivity of oxygen carrier in a fixed bed reactor was examined under alternating reducing and oxidizing conditions within the temperature range of 600–900 °C using fuel (50%  $\text{CO}$ , 50%  $\text{H}_2$ ) and oxidizing gas (steam). The results showed that this oxygen carrier has suitable reactivity that can produce hydrogen up to 90 molar percent in the product stream. It also led to a high conversion for oxidation and reduction phases when comparisons are made among 6 cycles. The cycle number had almost no effect on oxygen carrier reactivity after six cycles.

[F. Mahmoodi, S.H. Najibi, A. Shariati. **Hydrogen production via Chemical Looping Reforming using  $\text{Fe}_2\text{O}_3$  as oxygen carrier.** *J Am Sci* 2012;8(11):453-459]. (ISSN: 1545-1003). <http://www.jofamericanscience.org>. 70

**Keywords:** Global warming; Clean Fuel; Chemical looping water gas shift ; water splitting; Oxygen carrier;  $\text{H}_2$  generation.

### 1. Introduction

Hydrogen is a clean and efficient alternative to fossil fuels for the future. It is clean and has almost no negative impact on the environment, because water is its only combustion product (Chen et al, 2011; 2. Velazquez Vargas 2007).

Research activities on  $\text{H}_2$  production increase rapidly since it is an environmental friendly fuel that does not emit carbon dioxide which is known as one of the global warming gases (Schultz et al, 2003).

It is widely accepted today that carbon dioxide coming from fossil fuel combustion is the most important greenhouse gas contributing to global warming [de Diego et al, 2009]. The amount of carbon dioxide in the atmosphere is increasing continuously. Its accumulation in the air is one of the major causes of global warming and the change at equilibrium condition of weather and the environment (Kharaji et al, 2011).

There are limited options for hydrogen production without  $\text{CO}_2$  emissions. Hydrogen productions lead to the rise of emissions of  $\text{CO}_2$  and consequently increase the effect of greenhouse gaseous. Today hydrogen productions from natural gas lead to rise the emissions of  $\text{CO}_2$  and consequently increase the effect of greenhouse gaseous. One of the options to overcome anthropogenic greenhouse effect is the development of

$\text{CO}_2$  capture and storage (CCS) technologies (de Diego et al, 2009). CCS technology is recognized to be one of the most practical measures not disturbing economic activity, although this is a bridge-technology for the next generation where all energy sources are replaced by non  $\text{CO}_2$  emission resources (Kanai et al, 2012). The stabilization of atmospheric greenhouse gas concentrations cannot be reached without the  $\text{CO}_2$  capture. There are different  $\text{CO}_2$  capture technologies available for the carbon dioxide emissions. Some of these technologies are based on  $\text{H}_2$  production with  $\text{CO}_2$  capture [Ortiz et al, 2010]. It is likely that the production of  $\text{H}_2$  from the steam reforming of natural gas will be a dominant technology in the next few decades (Balasubramanian et al, 1999). In the conventional method like SMR due to pure Hydrogen,  $\text{CO}$  contaminants must be removed and separated from  $\text{H}_2$  (Chiron, 2011). The steam methane reforming process requires the Water Gas Shift (WGS) and Pressure Swing Adsorption (PSA) processes to produce pure hydrogen conventional. However, WGS is thermodynamically limited at high-temperature conditions and kinetically limited at low temperature conditions, which requires a two-stage process in industrial practice (Huffman et al, 2001). In contrast, the chemical looping based WGS process can be run at high temperature without thermodynamic constraints;

that is, it allows the inherent thermodynamic limitations of WGS to be overcome. In this process, the reaction is broken down into two half-reactions via chemical looping, in the first half-reaction, water is decomposed with oxidation of a metal oxide to produce  $H_2$  according to reaction 1. Alternatively, in the second half-reaction, synthesis gas reduces the metal oxide particles to produce  $CO_2$  and  $H_2O$  according to reaction 2. The reduced metal oxide is again used for first half reaction to be oxidized for the second half reaction. At complete conversion of the synthesis gas, the products from the first half reaction contains only  $H_2$  while from the second half reaction are  $CO_2$  and  $H_2O$ . Then  $CO_2$  is easily captured by condensation of  $H_2O$ . As can be seen the net reaction (reaction 3) is WGS reaction. The schematic diagram of this process is shown in figure 1.

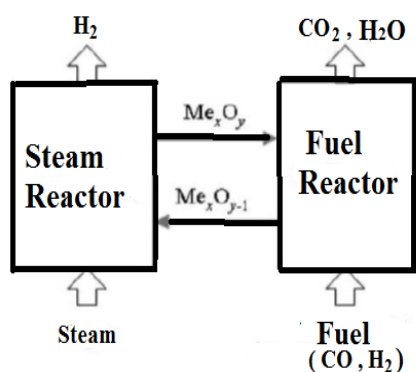
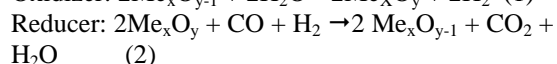
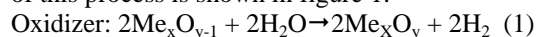


Figure 1: Conceptual diagram of Chemical Looping Reforming using Synthesis Gas.

The process can hence take full advantage of the fast reaction kinetics at high-temperature conditions. Since the steam/hydrogen stream is never contacted with the synthesis gas, the typical problems with CO contamination of the hydrogen effluent in WGS process are avoided, making additional purity of hydrogen stream. In this work, the activity of oxygen carrier ( $Fe_2O_3-CeO_2$ ) for  $CO_2$  capture via chemical looping reforming, using synthesis gas as fuel, at high temperature was investigated. The advantage of using iron oxide ( $Fe_2O_3$ ) as the oxygen carrier is that it does not involve catalytically dependent reactions (Gupta et al, 2007). Also  $Fe_2O_3$  is especially attractive since it also allows complete conversion of syngas as well as a high conversion of steam to hydrogen (Gupta, 2006). On the other hand  $Fe_2O_3$  also has the highest oxygen carrying capacity among all the other candidate metal oxides that have been studied in literature (Gupta,

2006). Supported  $CeO_2$  was added for extra stability and increasing iron oxide recyclability of the reactivity the oxygen carrier in multi cycles redox which is conceptually similar to that found by Gupta et al (Gupta, 2006) utilized  $TiO_2$  as support.

## 2. Experimental:

### 2.1 Synthesis of Oxygen Carrier:

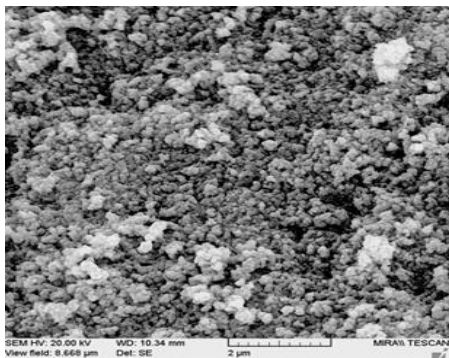
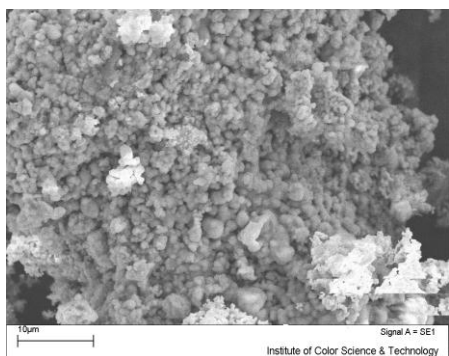
Oxygen carrier was prepared using co-precipitation method. Specifically,  $Ce(NO_3)_3 \cdot 6H_2O$ ,  $Fe(NO_3)_3 \cdot 9H_2O$  were weighed according to the desired Ce/Fe ratio. The salts were prepared in their solutions, respectively, and then mixed slowly in one beaker. The mixed solution was sufficiently stirred and heated at  $70^\circ C$ . A solution of 30% ammonia ( $NH_4OH$ ) was gradually added to the mixture with stirring when the pH value increased to 9 -9.5. Then, the resulting solution was maintained at  $70^\circ C$  with continuous stirring for 1.5 h. The precipitate thus obtained was aged for 5 h with the mother liquors, still under stirring at the reaction temperature and maintaining pH at 9 - 9.5. Then, the precipitate was filtered out and washed with successive portions of 400 ml of distilled water and ethanol (He et al, 2009). The paste mixture was dried at  $110^\circ C$  for 24 h after natural drying in the air overnight. Some dried gel-like material was obtained. This dried gel-like material was heated at  $300^\circ C$  for 2 h and was ground into powder. This powder was calcined in air at  $800^\circ C$  for 6 h. The main physical properties and composition of oxygen carrier are listed in Table 1.

Table 1: Result of BET test ( $Fe_2O_3-CeO_2$  as oxygen carrier)

Result of BET test	Unit	Quant
Single Point surface Area	$m^2/g$	23
BET Surface Area	$m^2/g$	22
BJH Desorption Cumulative Surface Area of Pores	$m^2/g$	30
Average Pore Diameter	A	411

### 2.2. Characterization of Oxygen Carrier:

To study the crystalline phase and chemical changes of oxygen carrier through the reaction, fresh and used oxygen carriers were analyzed by surface characterization techniques. The porous properties including BET surface area, pore volume, and average pore diameter were measured by nitrogen adsorption/desorption in ASAP test. The fresh and used oxygen carriers were also characterized by X-ray diffraction (XRD). Shape and morphology changes of the fresh and used oxygen carriers were studied by scanning electron microscopy (SEM).

Figure 2(a): SEM image of fresh  $\text{Fe}_2\text{O}_3\text{-CeO}_2$  particlesFigure 2(b): SEM image of reacted  $\text{Fe}_2\text{O}_3\text{-CeO}_2$  oxygen carrier after 5 cycles.

### 2.3 Experimental Setup:

The experiments were conducted in a fixed bed reactor with an online GC as shown in figure 3. The stainless steel 316 reactor had an inner diameter of 20 mm. The experimental system consisted of six sections, fixed bed reactor, temperature control unit, steam producer, mass flow control unit, a refrigerated cycle with a trap for condensing steam and gas analyzer. The reactor was placed in electric heater. The steam producer made of Armfield Engineering Equipment. The steam flow was controlled by adjusting the valve of water. The temperature of the oxygen carrier was monitored by a thermocouple placed in the center of the oxygen carrier bed. The flow rate of reducing gases was measured by Hitachi MFC.

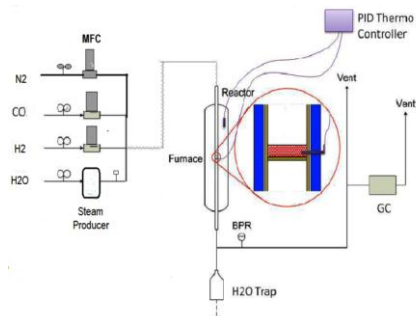


Figure 3: Schematic diagram of laboratory set-up reactor and gas analyzer

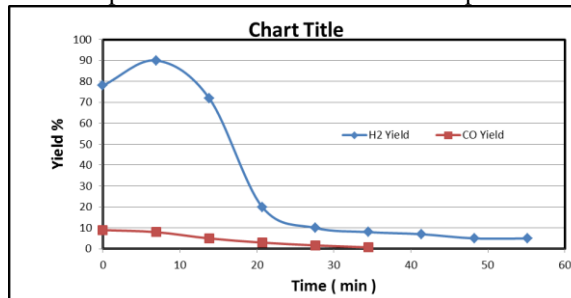
### 2.4 Experimental Procedure:

In each run, a sample of oxygen carrier (6 grams) particles was placed in the middle of the horizontal fixed bed reactor and hold by a porous plate. The bed height was approximately 20 mm. The reactor was heated to desired temperature under nitrogen atmosphere. The steam was then introduced to the reactor as oxidant to decompose at surface of oxygen carrier to produce hydrogen. The synthesis gases (50%  $\text{CO}$  and 50%  $\text{H}_2$ ) were injected to the reactor at a rate of 140 ml/min using two mass flow controllers. Between each phase of oxidation or reduction, pure nitrogen was introduced to the reactor for about 25 min to purge the reactants from the reactor. The products from the reactor were directed to the condensation trap, where the water was removed. Dried products were then sent to a gas chromatography (GC). The concentration of  $\text{H}_2$ ,  $\text{CO}$  and  $\text{CO}_2$  were analyzed by Young Lin GC. The GC detector was HID and its carrier gas was helium.

### 3. Result and discussion:

#### 3.1 Reactivity of $\text{Fe}_2\text{O}_3\text{-CeO}_2$ Oxygen Carrier in a Fixed Bed Reactor:

The gas product distribution of oxidation phase of the third redox cycle at  $700^\circ\text{C}$  is depicted in figure 4. The same distributions were obtained for the other cycles. This trend is similar to results in the literature where  $\text{Fe}_2\text{O}_3\text{-TiO}_2$  used in CLHG process (Chen et al, 2011). The main product of this phase is  $\text{H}_2$ . There are also some unreacted  $\text{H}_2\text{O}$  and some oxidized carbon deposited from reduction phase ( $\text{CO}$ ) in the exit gas stream. The yield of  $\text{H}_2$  leaving the reactor, in figure 4, is highest at initial stage of oxidation phase and then decreases as time proceeds.

Figure 4: Distribution of production gases from continuous fixed bed reactor at  $700^\circ\text{C}$  in oxidation cycle.  $\text{Fe}_2\text{O}_3\text{-CeO}_2 = 6$  gr.

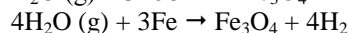
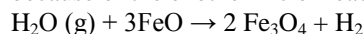
Some undesired product  $\text{CO}$  (concentration  $<9\%$ ) involved in  $\text{H}_2$  was detected. It is found that this undesired product ( $\text{CO}$ ) related to carbon formation on the oxygen carrier in reduction period. During steam oxidation,  $\text{CO}$  was detected in the hydrogen stream, indicating carbon deposition occurred in the reduction period similar results was found by Rahul et al (2010).

### 3.2 Effect of Temperature on Oxygen Carrier Reactivity

The effect of reaction temperature on oxygen carrier reactivity at the atmospheric pressure was studied. The temperature range in both reduction and oxidation phase was varied over a range of 600-900°C. All other operating conditions are the same as those stated in experimental section.

As can be observed the hydrogen production was decreased as temperature increased (see figure 5) which is conceptually similar to that found by Liang-Shih Fan (2010). In the chemical looping hydrogen generation system, there are two processes which have the potential to influence the hydrogen production, i.e., the reduction process and the steam oxidation process (Chen et al, 2011). Rate of Hydrogen production is about 0.64 (milli mole per min per gram of oxygen carrier particles).(mmol /min. gr <sub>O.C</sub>). However, the yield level of H<sub>2</sub> was decreased as temperature increased from 700 to 900°C. This behavior may be explained by studying the oxidation state and the characterization of fresh and used oxygen carrier.

According to figure 5, the rate of hydrogen in starting stage was higher at a lower temperature because of the exothermic of reactions



similar result was found by Shiyi Chen et al (2010).

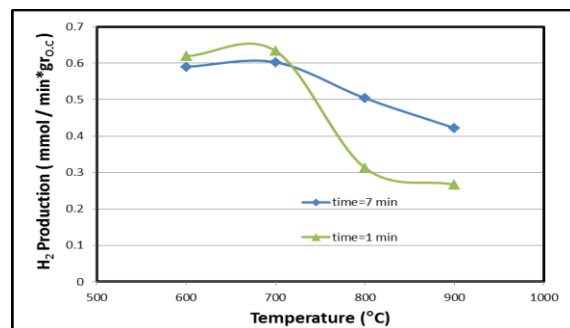
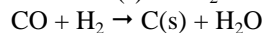
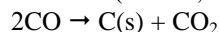


Figure 5: Effect of temperature on H<sub>2</sub> production at constant GHSV (GHSV=2500)

Generally, the carbon deposition on the surface of oxygen carrier can be presented by two reactions (Trimm, 1999)



These two reactions are favored at low temperature, lower than 700° C for reaction  $2\text{CO} \rightarrow \text{C(s)} + \text{CO}_2$  (Swierczynski et al, 2008). Therefore according to figure 6, because of the optimum temperature of reaction  $2\text{CO} \rightarrow \text{C(s)} + \text{CO}_2$  is 600 to 700°C so in this range of temperature Carbon dioxide produced per gram of oxygen carriers in minutes (mmol/min.gr <sub>O.C</sub>) is more than T=800°C but at

T=900° C Significant increase in this rate can be seen so the rate of CO<sub>2</sub> was increased as temperature increased from 800 to 900°C.

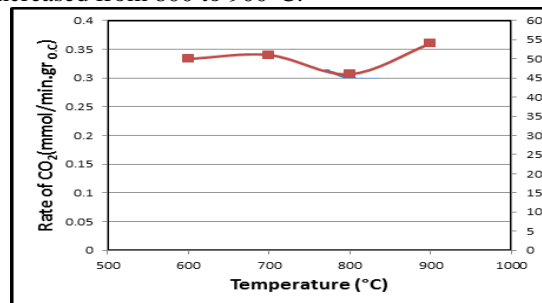


Figure 6: Effect of temperature on CO<sub>2</sub> production rate at constant GHSV (GHSV=2500)

### 3.3 Effect of Cycle Number on Oxygen Carrier Reactivity:

The yield of CO<sub>2</sub> at 700°C and various cycle numbers is shown in figure 7. All other operating conditions are the same as stated in experimental section. As shown in this figure, the peak of CO<sub>2</sub> production decreases with the cycle number. However, it remains constant after the 5<sup>th</sup> cycle. Generally For the early few cycles, rates of oxidation were slightly changed, but they were almost the same after the 5<sup>th</sup> cycle. Similar results were found by ishida et al (1999) which they investigated on performance of NiO as oxygen carrier. The results demonstrate that the reactivity of oxygen carrier was suitable after five cycles redox. As can be seen, the yield of CO<sub>2</sub> was more than 80% at some cycles. The result of this study suggests that higher cycle number results insignificant effect in oxygen carrier reactivity. The same behavior was also found for Hydrogen production in oxidation phase reaction.

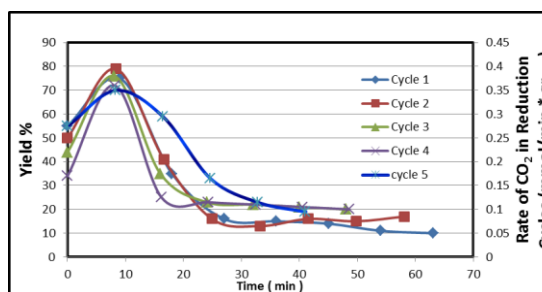


Fig. 7: Effect of cycle number at constant GHSV for rate of carbon dioxide in exhaust stream (T= 900°C) GHSV=2500 ml/h. gr <sub>O.C</sub>)

As result of figure 8, the peak of H<sub>2</sub> production decreases with the cycle number (the maximum peak for cycle 2, 3 and 4 are about 8 min but for cycle 4, 5,... are before 8 min) by comparing figure 7 and 8 it is likely that the initial cycle number

has slightly changed but oxidation and reduction cycles after 5<sup>th</sup> cycle very similar to each other.

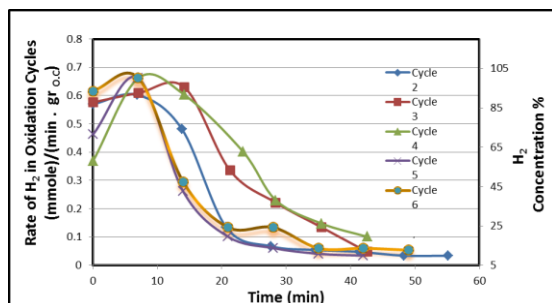


Figure 8: Effect of cycle number at constant GHSV for rate of Hydrogen generation (T= 700°C) GHSV=2500 ml/h.gr oc)

As can be seen in figure 7 and 8 rate of the gaseous production can be regarded as a function of cycle number in reduction and oxidation period. The results demonstrate the reactivity of oxygen carrier was suitable after five cycles redox.

### 3.4 Characterization of Fe<sub>2</sub>O<sub>3</sub>-CeO<sub>2</sub> Oxygen Carrier:

The XRD and XRF analysis of fresh and used oxygen carrier are shown in figure 9, and tabulated in tables 3 and 4. As shown in figure 9(a), It is observed that Iron oxide (Fe<sub>2</sub>O<sub>3</sub>) was well deposited on the surface of CeO<sub>2</sub>. Fresh oxygen carrier consists only two crystal phases, Fe<sub>2</sub>O<sub>3</sub> and CeO<sub>2</sub>. Thus, a limited interaction between the metal oxide and CeO<sub>2</sub> occurred during the sintering. As shown in the XRD picture in figure 9(b), after six redox cycle at 700°C, The reacted oxygen carrier consists four phases, including CeFeO<sub>3</sub>, CeO<sub>2</sub>, Fe<sub>3</sub>O<sub>4</sub> and Fe<sub>2</sub>O<sub>3</sub>, although no significant chemical changes have occurred in the solid phase during the experiments. Similar result were found by ZHU Xing et al (2010). On the basis of their experimental results, the cerium orthoferrite (CeFeO<sub>3</sub>) can be prepared by the reaction  $3\text{CeO}_2 + \text{Fe}_2\text{O}_3 + \text{Fe} \rightarrow 3\text{CeFeO}_3$  at 800-850°C (Soo et al, 2010). However, our experiment was done at 700°C and used Synthesis gas as reformer gas. This may explain the difference in findings, since in this study the mixture (CeO<sub>2</sub> and CeFeO<sub>3</sub>) was obtained. ZHU Xing et al found characteristic peaks of CeFeO<sub>3</sub> gradually increasing from the first cycle to the 10th cycle (Xing et al, 2010). Results of this study show that the formation of iron cerium oxide is most probably explained by the reaction between the active phase and support during the reduction cycle. Figure 9(c) is shown crystalline phase after oxidation period. XRD analysis revealed that the oxygen carrier particle can be completely oxidized or reduced during the multicycle chemical looping reforming. To find the optimum reduction temperature for oxygen carrier, the TPR test was carried out. The results are depicted in

figure 12 It is shown that there are three reduction peaks with a shoulder peak in the TPR profile. It is also found that these three reduction peaks appeared at 415°C, 561°C and 738°C and assigned to the reduction of Fe<sub>2</sub>O<sub>3</sub> to Fe<sub>3</sub>O<sub>4</sub>, Fe<sub>3</sub>O<sub>4</sub> to FeO, and FeO to Fe metal, respectively (Xing et al, 2010). The first peak at the lower temperature according to XRD results must be assigned to Fe<sub>3</sub>O<sub>4</sub> reduction, although it appears shifted by about 700°C toward the higher temperature with reference to bulk TPR profile of cerium supported iron oxide as oxygen carrier. The second peak may be owing to the contribution of reduction of lattice oxygen in CeO<sub>2</sub> and CeFeO<sub>3</sub> (Xing et al, 2010). The TPR results show that the Fe<sub>2</sub>O<sub>3</sub>-CeO<sub>2</sub> is most easily reduced.

Table 2: Result of XRF test (fresh and used Fe<sub>2</sub>O<sub>3</sub> - CeO<sub>2</sub> as oxygen carrier after 5 cycle redox)

Result of XRF test (Fresh and used particles)	Fresh	Used
	%	
Fe <sub>2</sub> O <sub>3</sub>	37.95	31.89
CeO <sub>2</sub>	61.03	44.51
Al <sub>2</sub> O <sub>3</sub>	0.38	0.1
SiO <sub>2</sub>	0.1	5.1
MgO	0.02	4.76

According to **table 3**, XRF result shows percentage of oxygen carrier particles after reaction is about 85%, so it is deduced that the other percent related to CeFeO<sub>3</sub> that XRF test couldn't to detect it.

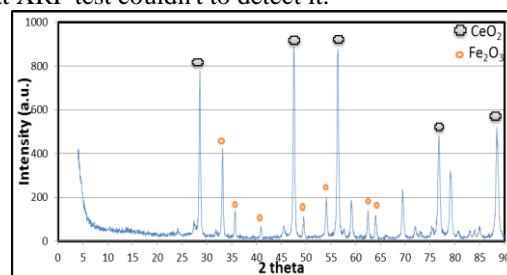


Figure 9(a): XRD characterization of fresh iron oxide on CeO<sub>2</sub> as support.

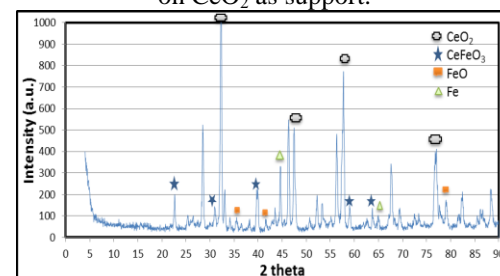


Figure 9(b): XRD characterization of reacted iron oxide on CeO<sub>2</sub> as support after 5 cycle redox.

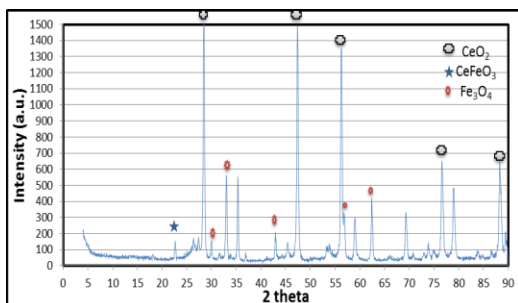


Figure 9(c): XRD characterization of reacted iron oxide on CeO<sub>2</sub> as support after oxidation cycle.

Table 2: XRD result of fresh and used Fe-Ce-O particle prepared by co precipitation method

XRD	Crystalline phase			
	Major phase after 5 <sup>th</sup> cycle Reduction	Minor phase after 5 <sup>th</sup> cycles Reduction	Major phase after 5 <sup>th</sup> cycle oxidation	Minor phase after 5 <sup>th</sup> cycle oxidation
Fe <sub>2</sub> O <sub>3</sub> CeO <sub>2</sub>	CeFeO <sub>3</sub> CeO <sub>2</sub> Fe	FeO Fe <sub>3</sub> O <sub>4</sub> Fe <sub>2</sub> O <sub>3</sub>	CeO <sub>2</sub> Fe <sub>3</sub> O <sub>4</sub>	FeO

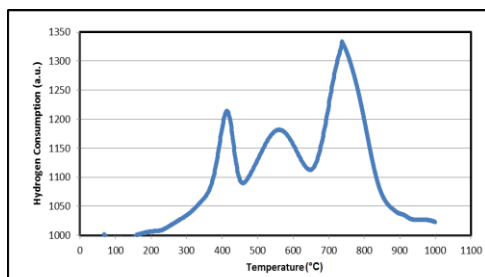


Figure 10: TPR profile of Fe<sub>2</sub>O<sub>3</sub>-CeO<sub>2</sub> were made by co-precipitation method.

Surface of Fe<sub>2</sub>O<sub>3</sub>-CeO<sub>2</sub> oxygen carrier was studied before and after the reaction with a SEM, as result of figure 2(a) and 2(b), no major differences were found between fresh and reacted particles, the surface of the particles appeared rougher and more porous. As shown in the SEM image, carbon grows from iron and develops on one side of the particles. At figure 2b the micrograph shows two distinct regions which appears as bright and dark gray, this kind of morphology was named "moss-like" carbon by Matsukata et al (1996).

### 3. Conclusion:

Pure hydrogen can be produced by some processes to be used in downstream applications such as fuel cell. Chemical looping reforming is such a process which produces pure hydrogen and at the same time does not allow the mixing of CO<sub>2</sub> with it making an inherent CO<sub>2</sub> capture. In this study, reactivity of Fe<sub>2</sub>O<sub>3</sub>/CeO<sub>2</sub> as oxygen carrier was found to be suitable for the

chemical looping reforming since it produces 90% H<sub>2</sub> on a volume basis in a completely separate gas stream. Results of multi-cycle reduction/oxidation reactions showed that Fe<sub>2</sub>O<sub>3</sub>/CeO<sub>2</sub> particles are stable in seven cycles. Reaction temperature showed a minor effect on structure of Fe<sub>2</sub>O<sub>3</sub>/CeO<sub>2</sub> oxygen carrier according to XRD and SEM test. Fe<sub>2</sub>O<sub>3</sub>/CeO<sub>2</sub> as oxygen carrier also showed high activity and stable behavior over multi redox cycles in the temperature range from 700 to 900°C.

### Acknowledgments:

The authors kindly acknowledge the support provided by the Iranian Nano Technology Initiative Council and the scientific association of Petroleum University of Technology.

### Corresponding Author:

Dr. A. Shariati  
Department of Gas Engineering  
Petroleum University of Technology  
E-mail: [shariati@put.ac.ir](mailto:shariati@put.ac.ir)

### References:

- Balasubramanian, B.; Lopez Ortiz, A.; Kaytakoglu, S.; Harrison, D. P, "Hydrogen from methane in a single step process," Chem. Eng. Sci, 54, 3543-3552 (1999).
- Chen S, Qiliang Shi, Zhipeng Xue, Xiaoyan Sun, Wenguo Xiang, "Experimental investigation of chemical-looping hydrogen generation using Al<sub>2</sub>O<sub>3</sub> or TiO<sub>2</sub>-supported iron oxides in a batch fluidized bed," International journal of hydrogen energy, 36, 8915 -8926 (2011).
- Chen, S., W. Xiang, Z. Xue and X. Sun; "Experimental investigation of chemical looping hydrogen generation using iron oxides in a batch fluidized bed," Proceedings of the Combustion Institute, 33, 2691–2699 (2011).
- Chiron F X, Gregory S. Patience, Se bastien Riffart, "Hydrogen production through chemical looping using NiO/NiAl<sub>2</sub>O<sub>4</sub> as oxygen carrier," Chemical Engineering Science, 66, 6324–6330 (2011).
- de Diego L F, María Ortiz, Francisco García-Labiano, Juan Adánez, Alberto Abad, Pilar Gayán, "Hydrogen production by chemical-looping reforming in a circulating fluidized bed reactor using Ni-based oxygen carriers," Journal of Power Sources, 192, 27–34 (2009).
- Fan, L. S.; "Chemical Looping Systems For Fossil Energy Conversions," A John Wiley and Sons, Inc, 2010, publication page 224 and 239
- Gupta P, Velazquez-Vargas LG, Fan L-S, "Syngas redox (SGR) process to produce hydrogen from coal

- derived syngas," *Energy & Fuels*, 21, 2900–2908 (2007).
8. Gupta P, "Regenerable Metal Oxide Composite Particles and Their Use in Novel Chemical Processes," Doctoral thesis of The Ohio State University 2006, page 40, 162, 202
  9. He F., Y. Wei, H. Li, and H Wang; "Synthesis Gas Generation by Chemical-Looping Reforming Using Ce-Based Oxygen Carriers Modified with Fe, Cu, and Mn Oxides," *Energy & Fuels*, 23, 2095–2102 (2009).
  10. Huffman G, Wender I, "Fuel science in the year 2000: an introduction," *Fuel Process. Technol.*, 71, 1-3 (2001)
  11. Ishida M, Jin H, and Toshihiro Okamoto., "Development of a Novel Chemical Looping Combustion: Synthesis of a Solid Looping Material of NiO/NiAl<sub>2</sub>O<sub>4</sub>," *Ind. Eng. Chem. Res.*, 38, 126-132 (1999).
  12. Kanai, Y., K. Terasaka, M. Suwabe, S. Fujioka and D. Kobayashi; " Development of Slurry Bubble Column with Lithium Silicate to Recover Hot CO<sub>2</sub> from flue Gas," *journal of chemical engineering of Japan*, 45, 639-644 (2012).
  13. Kharaji A G, A. Shariati, M.A. Takassi, "Selectivity and Performance of Fe-V<sub>2</sub>O<sub>5</sub>/γ-Al<sub>2</sub>O<sub>3</sub> Nano Catalyst for Methanol Production with Reverse Water Gas Shift (RWGS) Reaction," *Journal of American Science*, 7(12), 1064-1068 (2011)
  14. Matsukata M., Matsushita T, Ueyama K., "A novel hydrogen/syngas production process catalytic activity and stability of Ni/SiO<sub>2</sub>," *Chemical Engineering Science*, 51, 2769–2774 (1996)
  15. Ortiz M., L. F. Diego, A. Abad, F. García-Labiano, P. García, J. Adánez; "Hydrogen production by auto-thermal chemical-looping reforming in a pressurized fluidized bed reactor using Ni-based oxygen carriers," *International journal of hydrogen energy*, 35, 1511–160 (2010).
  16. Rahul D. Solunke and Gotz Vesper, "Hydrogen Production via Chemical Looping Steam Reforming in a Periodically Operated Fixed-Bed Reactor," *Ind. Eng. Chem. Res.*, 49, 11037–11044 (2010).
  17. Schultz MG, Diehl T, Brasseur GP, Zittel W, "Air pollution and climate forcing impacts of a global hydrogen economy," 302, 624–627 (2003).
  18. Soo K K, Kim Chang Hee, Bae Ki kwang, Cho Won Chul, Kim Woo Jin, Kim Young Ho, Kim Sung Hyun, Park Chu Sik, "Redox cycling of CuFe<sub>2</sub>O<sub>4</sub> supported on ZrO<sub>2</sub> and CeO<sub>2</sub> for two-step methane reforming/water splitting," *Int. J. Hydrogen Energy*, 35, 568-576 (2010).
  19. Swierczynski D C, Courson, A. Kiennemann. Study of steam reforming of toluene used as model compound of tar produced by biomass gasification. *Chem Eng Process*, 47, 508–513 (2008)
  20. Trimm DLA. Catalysts for the control of coking during steam reforming. *Catal Today*, 49, 3–10 (1999)
  21. Velazquez Vargas, L. G.; "Development Of Chemical Looping Gasification Processes For The Production Of Hydrogen From Coal," Presented in Partial Fulfillment of the Requirements for the Degree Doctor of Philosophy in the Graduate School of The Ohio State University, page 131 (2007).
  21. ZHU Xing, WANG Hua, WEI Yonggang, LI Kongzhai, CHENG Xianming, "Hydrogen and syngas production from two-step steam reforming of methane over Fe<sub>2</sub>O<sub>3</sub>-CeO<sub>2</sub> oxygen carrier," *Journal of Rare Earths*, 28, 907 (2010).

10/12/2012